Power Doppler ultrasound scan imaging of the level of red blood cell aggregation: An in vitro study

Louis Allard, MSc, and **Guy Cloutier, PhD,** *Montréal, Canada*

Purpose: **The purpose of this study was to evaluate the effect of the shear rate on red blood cell (RBC) aggregation with power Doppler ultrasound scanning (PDU), pulsed-wave Doppler scanning, and color Doppler flow imaging.**
Methods: **Equine and porcine blood were circulated with a steady flow in a phantom with a diameter of 9.52 mm. The color Doppler flow imaging mode was used to estimate the velocity profile and the shear rate across the tube. A transfer function that related the Doppler scan power, measured in gray level with the PDU method, to the power, measured in decibels with the pulsed-wave Doppler scan technique, was used to estimate the echogenicity of blood and the level of aggregation.**
Results: **For the four experiments reported, the power peaked at low shear rates probably because of increased RBC collisions and aggregation and then decreased thereafter because of disaggregation. The largest power variations were measured at shear rates of less than 40 seconds^{-1}. At flow rates that varied between 75 and 500 mL/min, the echogenicity was low near the wall of the tube, increased toward the middle, and decreased at the tube center. The Doppler scan power was uniform across the tube at flow rates of 750 and 1000 mL/min.**
Conclusion: **PDU is reliable to quantify the echogenicity of blood and the level of RBC aggregation. In comparison with other methods proposed to measure RBC aggregation, ultrasound scanning is applicable in vivo and may help to improve our basic understanding of the relationship between the hemodynamic of the circulation and RBC aggregation in human vessels. (J Vasc Surg 1999;30:157-68.)**

Power Doppler ultrasound scan (PDU) is an imaging method that displays the power of the Doppler scan blood flow signal.[1] This technique is used to image low flow in the microvasculature and to assess areas of ischemia and hyperemia in cases of inflammation. In large vessels, this noninvasive imaging technique was proposed to grade arterial stenoses[2,3] and to detect intracranial aneurysms.[4] Results comparable with x-ray angiography and superior to color Doppler flow (CDF) imaging were obtained. In addition to the clinical applications mentioned previously, other uses of this technique may emerge. More specifically, PDU may allow the quantification of blood flow turbulence[5,6] and the level of red blood cell (RBC) aggregation.[7,8]

With pulsed-echo A-mode ultrasound scan systems, experimental studies showed that the power backscattered by blood depends on many factors, such as the volume of the scatterers (RBCs and RBC aggregates), the hematocrit, the frequency of the ultrasound scan signal, the concentration of plasma proteins that affect RBC aggregation, and the flow condition.[9] Among these factors, the shear force affecting the size of RBC aggregates is the most important under flowing in vivo condition, if measurements are performed at a fixed transmitted frequency. Theoretically, at a constant hematocrit, the power backscattered by a suspension of scatterers is proportional to their volume when they are small enough to respect the Rayleigh scattering condition. Although the exact relationship between the Doppler scan power and the RBC aggregate size,

From the Laboratory of Biomedical Engineering, Institut de recherches cliniques de Montréal, and the Faculty of Medicine (Dr Cloutier), Université de Montréal.
This work was supported by a research scholarship from the Fonds de la Recherche en Santé du Québec (G. C.), and by grants from the Medical Research Council of Canada (#MT-12491) and the Heart and Stroke Foundation of Quebec.
Reprint requests: Dr Guy Cloutier, Institut de recherches cliniques de Montréal, 110 avenue des Pins ouest, Montréal, Québec, Canada, H2W 1R7.

0741-5214/99/$8.00 + 0 24/1/97708

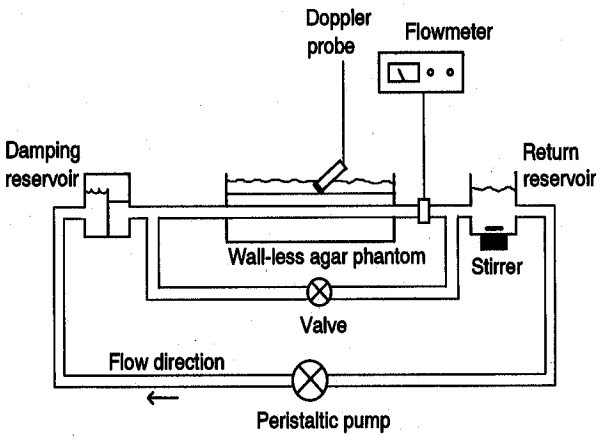

Fig 1. Schematic representation of steady flow loop model.

shape, and packing organization is not well understood, the current knowledge suggests that the power is proportional to the mean volume of the aggregates.[8] The objective of this study was to show the feasibility of PDU to assess the effect of the shear rate on the level of RBC aggregation. The shear rate within the flow model was estimated from the two-dimensional (2D) velocity distribution measured with CDF imaging.

MATERIALS AND METHODS

Flow loop model and experimental protocol. Experiments were performed at room temperature in a horizontal steady flow loop model illustrated in Fig 1. The phantom contained a tissue-mimicking material and a wall-less vessel with a diameter of 9.52 mm. The tissue mimic made of distilled water mixed with high-strength agar gel (3%) and glycerol (8%) had an acoustic velocity similar to that of soft tissue. The wall-less vessel was formed by pouring the molten tissue mimic around a rod that was removed after the tissue mimic set. The phantom did not absorb water, and the vessel lumen maintained its original shape over time. The phantom was kept in a water bath between experiments to avoid drying of the gel and possible deformation. More details on how the phantom was made can be found in Rickey et al.[10] The inlet length of the flow model was straight and long enough to ensure a fully developed laminar flow at the recording site for all flow rates used in the study (inlet length/vessel diameter of about 120).[11] A reservoir of 1 L allowed the filling of the model with blood. A magnetic stirrer was used to prevent sedimentation in the reservoir and to maintain a uniform concentration of scatterers throughout the test fluid. A peristaltic pump circulated the blood at different flow rates. Any flow oscillations produced by the pump were eliminated with the use of a damping filter located between the pump and the test section (Fig 1). The flow rate was continuously measured with a cannulating type flow probe coupled to an electromagnetic flowmeter (Cliniflow II, model FM701D, Carolina Medical Electronics, King, NC). The pressure was not monitored in the flow model.

An Advanced Technology Laboratories Ultramark 9 HDI ultrasound scan system (Bothell, Wash), with a 38-mm aperture, 4-MHz linear array probe (L7-4), was used to produce cross-sectional color Doppler scan images (velocity and power modes). Water allowed acoustic coupling between the probe and the agar phantom. The angle between the probe and the axis of the tube was 60 degrees. For all measurements, the image sensitivity of the ATL system was 16, the persistence was 7, and the dynamic image filtering option was not activated. The system was operated in zoomed high resolution mode, with the transmitting focal point set near the center of the tube at a depth of about 3.5 cm. Because a gray-scale video frame grabber system was used to digitize Doppler scan images, a gray-scale map was selected to display the velocity and the power information on the ATL. The image acquisition system was on the basis of a Power Macintosh 7500 computer (Life Imaging System Inc, London, Ontario, Canada). The video images had a dimension of 256 × 256 pixels and were digitized with a precision of 8 bits/pixel. The resulting pixel resolution of the images was determined by positioning successively two cursors in the x and y directions on the ATL screen and by measuring their respective distance in millimeters and pixel number.

Four experiments that were performed under steady flow with porcine and equine whole blood are reported. Several other experiments were done before the final protocol, and these are not included in the current report. Porcine and equine blood species were used to mimic normal and pathologic RBC aggregation levels.[12] For each experiment, six flow rates (75, 125, 250, 500, 750, and 1000 mL/min) were chosen to cover a wide range of shear rate. The fresh blood collected from an abattoir was anticoagulated with ethylenediamine tetraacetic acid and was adjusted to 40% hematocrit by remixing the plasma with the RBCs and buffy coat separated by sedimentation. The blood was kept at 4°C before measurements performed within 2 days of collection.

For each blood sample, the level of RBC aggregation was assessed at room temperature the day of the experiment, with a previously validated erythroaggregameter on the basis of a Couette flow arrangement (Regulest, Florange, France).[13,14] The following three RBC aggregation indices were provided by the instrument: the primary aggregation time (tA in seconds), the aggregation index at 10 seconds (S_{10}, no unit), and the total dissociation threshold (γS in seconds^{-1}), measured with the analysis of the variations in light intensity of the signal scattered by blood. The indices tA and S_{10} give information on the kinetics of rouleau formation as a function of time. A blood sample whose RBCs aggregate quickly will have a small value of tA, whereas RBCs, which aggregate very little, will display large tA values. The index S_{10} is proportional to the level of aggregation. Measurements performed as a function of the shear rate allowed the determination of γS, which corresponds to the minimum shear rate at which RBCs are completely dissociated. The parameter γS is proportional to the adhesive strength between RBCs.

Cross-sectional distribution of the Doppler scan power, velocity, and shear rate. For all power Doppler scan image acquisitions, the pulse repetition frequency (PRF) was set to 1500 Hz and the wall filter was 50 Hz. Flow velocities below 1.9 cm/s were removed with the wall filter. The PRF was chosen high enough (1500 Hz) to avoid frequency aliasing artifacts on the images (Appendix). To compare power measurements from a given animal, it was important to keep the Doppler scan gain and the energy of the transmitted echoes constant for all flow rates. The optimal setting should avoid any image saturation in the presence of large RBC aggregates (at low shear rates) and produce an adequate signal-to-noise ratio when imaging disaggregated RBCs (at high shear rates). Because of the variations in echogenicity between blood samples and the limited range of power that can be displayed by the instrument, the Doppler scan gain could not be kept constant between animals.

For each Doppler scan velocity distribution, the lowest PRF that avoided frequency aliasing was chosen to display the image over the full range of the velocity scale. For a given flow rate, the Doppler scan gain and the transmitted power were selected to obtain images that matched the cross-sectional area of the tube displayed in B-mode. Modifications of these parameters were necessary when changing the flow rate because the instrument automatically changes the energy of the transmitted echoes when modifying the PRF. For a given PRF, the lowest wall filter frequency available was chosen in Doppler scan velocity mode.

To evaluate the Doppler scan power and velocity distributions as a function of the radial position within the tube, 128 frame-grabbed video images were digitized and averaged. During digitization, the B-mode gain was set to zero to reject all tissue data. The mean images were resized by considering the Doppler scan angle to obtain a circular cross-section instead of an ellipsoid. From the mean distribution, the center of the tube was determined by computing the center of gravity of the 2D vessel lumen segmented manually to remove the background noise. From this central position and with the assumption of a 2D radial symmetry, the 2D power Doppler scan distribution P(x,y) was reduced to a 1D power profile P(r) by transforming the Cartesian coordinate system to a polar system. Similar transformations were used to obtain the 1D velocity profile V(r) from the 2D distribution V(x,y). Each pixel gray level of the mean velocity image, V(x,y), was converted into velocity with the gray scale-to-velocity transfer function described in the next section. The functions P(r) and V(r) were evaluated at increments of 0.5 mm.

To determine the shear rate as a function of the radial position within the tube, the velocities V(r) were fitted to the power law model given by:

$$(1)\quad v(r) = v_{max}\,[1 - (r/R)^n]$$

where v_{max} is the maximum centerline velocity, r is the distance from the center of the tube in increments of 0.5 mm, R is the radius of the tube, and n is the power law exponent. For a parabolic velocity profile, n is 2, and it is greater than two for a blunt profile. On the basis of the Marquardt-Levenberg least-square algorithm (SigmaPlot for Windows, ver. 1.02, Jandel Scientific, San Rafael, Calif), the value of the parameter n was found from the curve-fitting model of Equation 1. Although the tube radius was known, the experimental value of R was also determined with the curve-fitting model to simulate more realistic in vivo conditions where the radius would be difficult to evaluate precisely on the B-mode image. As a result of the lower accuracy in estimating blood velocities near the wall, the velocities recorded at a radial position greater than 4 mm were not considered in the curve fitting. By computing the derivative $\partial v(r)/\partial r$ of Equation 1, the shear rate $\gamma(r)$ was calculated by:

$$(2)\quad \gamma(r) = n v_{max} r^{(n-1)}/R^n$$

Transfer function of the gray scale-to-velocity mapping. For CDF imaging, the transfer function between the gray level and the velocity was determined by taking into account nonlinearities in the

gray scale defined by the instrument. Each level of the gray scale, gray(j), was linearized by converting its value at the position j to a velocity at the new position i. The velocity was assigned to this new position, as described in Equation 3. To do that, the color bar was digitized and the intensity of each gray level was determined with the Photoshop software (Adobe Systems Inc, ver. 3, Mountain View, Calif). On the basis of a linear velocity range defined between 0 m/s and $V_{prf/2} = (PRF \times c)/[4 \times F_t \times \cos(\theta)]$, where c is the speed of sound in blood (1570 m/s), F_t is the transmitted ultrasound frequency, and θ is the Doppler scan angle, each gray level of the color bar was transformed to a velocity $V_{gray(i)}$ by computing:

$$(3)\quad V_{gray(i)} = V_{prf/2} \times (i - 1)/(N - 1), \text{ for } i = 1, 2, \ldots, N,$$

where i is the i^{th} position on the color bar and N is the total number of levels of the color bar, which is 16 for the instrument settings that were used. From this equation, the velocity associated to each pixel of the averaged 2D-velocity distribution was computed with linear interpolation. In Equation 3, $V_{prf/2}$ was used instead of the maximum velocity displayed at the top of the color bar because this value is rounded off at low flow velocities.

Transfer function of the gray scale-to-power mapping. For mapping the Doppler scan power, the ATL ultrasound system uses 14 discrete values of gray level, ranging from 16 (background) to 224 (saturation). However, because PDU was developed to provide noninvasive angiographic images, the relationship between the gray level and the backscattered power is compressed and highly nonlinear. As a consequence of that, quantitative power measurements with this technique are difficult. A calibration procedure is proposed to determine the transfer function between the gray level of PDU images and the backscattered power in decibels. As shown by others,[15] the backscattered power from small particles is linear at low particle concentrations. This observation was used to calibrate the backscattered power in decibels. Superfine Sephadex particles (Sigma Chemical, no G25, Oakville, Ontario, Canada) were suspended in a mixture of 70% water and 30% glycerol and were circulated in the flow model at a flow rate of 350 mL/min. Different concentrations, ranging from 1 g/L of the solution to 0.0039 g/L, were obtained with dilution. These concentrations corresponded to hematocrits, ranging from 0.5% to 0.002%, approximately. For each concentration, PDU images were recorded to obtain the mean gray level, and pulsed-wave (PW) Doppler scan measurements were performed to measure the backscattered power in decibels.

The acquisition of the PW Doppler scan signals was performed during 10 seconds with a Data Translation acquisition board (Transduction Inc, model DT-2828, Mississauga, Ontario, Canada). The sampling frequency was chosen high enough (3 kHz) to avoid frequency aliasing. The Doppler scan sample volume was positioned at the center of the tube, and it had an axial dimension of 1 mm. The transmitted PW Doppler scan power and the output gain of the imaging system were kept constant for all measurements performed at different Sephadex concentrations. For PDU, the acquisition was performed at three different levels of Doppler scan gain (50%, 40%, and 30%) to determine whether the transfer function was influenced by the gain setting. The transmitted power in power mode was constant for all Sephadex concentrations. For each measurement, 128 cross-sectional PDU images of the vessel lumen were digitized and averaged. The mean gray level was estimated from a region of interest having approximately the same size (1 mm^2) and located at the same position as the PW sample volume. Besides the transmitted power and Doppler scan gain, all other PDU settings were constant and the same as given previously. The conversion of the PDU Doppler scan power from gray levels to decibels was obtained with linear regression for each gain setting.

RESULTS

Calibration and validation of the technique. Fig 2 shows the transfer function of the gray scale-to-power mapping performed with the ATL system. Logarithmic relationships were found between the gray level and the concentration of Sephadex for the three output gains tested. The gray level that corresponded to the saturation of the power Doppler scan mean image increased with the output gain, and the range of power that could be displayed did not seem to be affected by the selection of this parameter. For a gain of 50%, the saturation of the image corresponded to the maximum gray level that could be measured (ie, 224). As expected, measurements performed with the PW Doppler scan technique showed a linear relationship between the backscattered power and the concentration of Sephadex (results not shown). Similar results were obtained previously in another study.[16] To quantify the intensity of the PDU images, the Doppler scan power in gray level was expressed as a function of the PW Doppler scan power in decibels. As seen in Fig 3, linear relationships were found for all gain settings. On

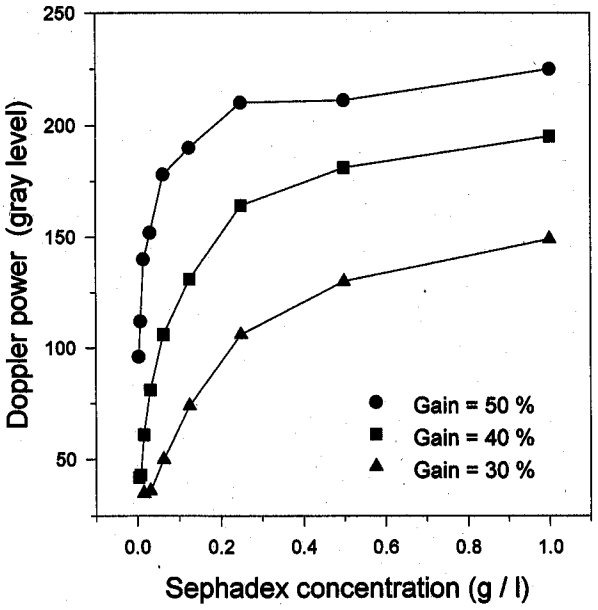

Fig 2. Transfer functions of gray scale-to-power mapping that characterizes Advanced Technology Laboratories instrument for three different output gains of 50%, 40%, and 30%. Mean power Doppler scan intensity in gray level was measured at center of tube for Sephadex concentrations varying between 0.0039 g/L and 1 g/L.

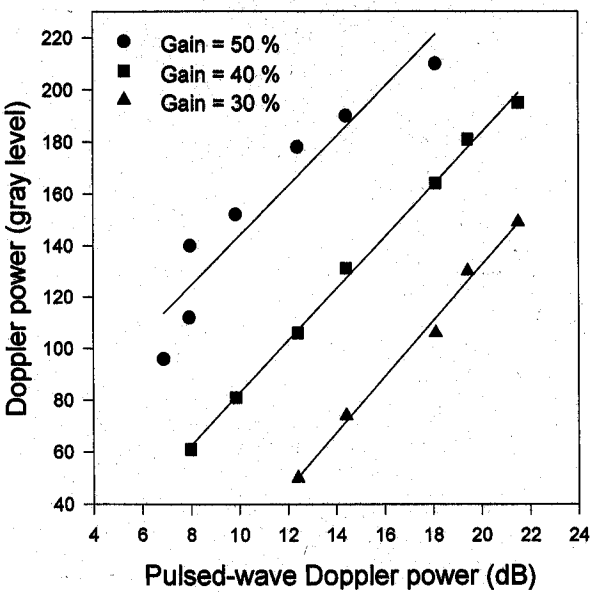

Fig 3. Linear regressions between Doppler scan power (gray level), measured with power Doppler ultrasound scan technique, and pulsed-wave Doppler scan power for output gains of 50%, 40% and 30%. Sephadex particles were circulated in flow model at concentrations varying between 0.0039 g/L and 0.25 g/L. Mean slope of three regression lines was 10.6 ± 0.4 gray level/dB (r^2 = 0.96 ± 0.06). This slope was used to convert power Doppler ultrasound scan measurements with blood in decibels.

the average, the slope of the three regression lines was 10.6 ± 0.4 gray level/dB (r^2 = 0.96 ± 0.06). This slope was used to convert PDU measurements with blood in decibels. On the basis of this slope, the range of the gray scale (16 to 224) was linearly represented between 1.5 and 21.3 dB.

Measurements with porcine and equine whole blood. Table I summarizes the aggregation indices measured with the erythroaggregameter for the series of four experiments reported in this study. The kinetics of rouleau formation, which is proportional to S_{10} and inversely proportional to tA, was more important for horse blood than for pig blood. The adhesive strength between RBCs (γS) was also higher in horse blood.

Fig 4 shows examples of the 2D power Doppler scan distribution obtained with horse blood at low (75 mL/min) and high (1000 mL/min) flow rates. These two images were not corrected for the Doppler scan angle, were averaged over 128 frames, and were produced with the same instrument settings. The highest intensity and the smaller area were obtained at a flow rate of 75 mL/min. At that flow rate, the mean gray level was 112 ± 54 and the tube area was 52.9 mm² (area without correction for the Doppler scan angle). At a flow rate of 1000 mL/min, the mean gray level was 35 ± 7 and the tube area was 73.8 mm². The smaller area observed at a flow rate of 75 mL/min was caused by the effect of the wall filter. An interesting observation can be made on Fig 4 at a flow rate of 75 mL/min. A reduction of the backscattered power was found at the center of the tube. This power drop, known as the "black hole" phenomenon,[17] was first observed

Table I. Red blood cell aggregation indices measured with the erythroaggregameter for the series of four experiments performed with equine and porcine whole blood

Aggregation indices	*Horse (1)*	*Horse (2)*	*Pig (1)*	*Pig (2)*
tA (seconds)	1.6	1.8	4.2	4.8
S_{10}	29	26	12	9.5
γS (seconds^{-1})	300	345	75	55

tA, Primary aggregation time; S_{10}, aggregation time at 10 seconds; γS, total dissociation threshold.

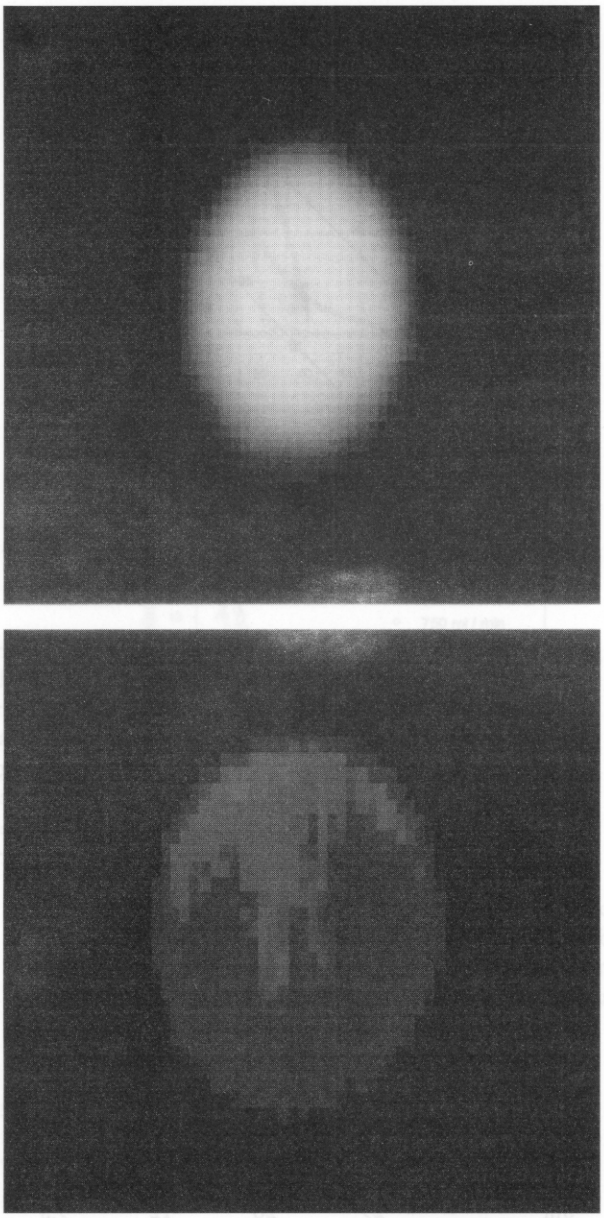

Fig 4. Examples of two-dimensional power Doppler scan distribution obtained with horse blood (horse 1) at flow rates of 75 mL/min *(top)* and 1000 mL/min *(bottom)*. These two images (256 × 256 pixels) were obtained by averaging 128 video frames with x-y resolution of 0.0724 × 0.0645 mm/pixel, respectively. The Doppler scan angle was 60 degrees, and ultrasound scan instrument settings were the same for both images.

on B-mode images of porcine whole blood circulated in a large diameter tube (2.54 cm). In the present study, the "black hole" was seen for both porcine and equine bloods at flow rates equal or lower than 250 mL/min.

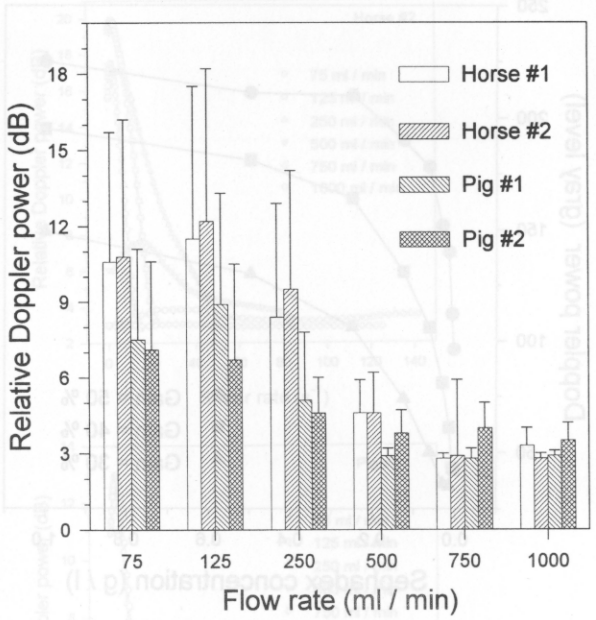

Fig 5. Doppler scan power averaged across vessel lumen of mean power Doppler ultrasound scan images as function of flow rate for four experiments performed with equine and porcine whole blood. *Error bars* represent standard deviations of Doppler scan power computed from all pixels within vessel lumen. *Error bars* do not reflect reproducibility of results, but they indicate range of variation of RBC aggregation level across tube. Because different transmitted power and Doppler scan gain were used to produce ultrasound scan images of each blood sample, absolute value of power in decibels cannot be compared between animals.

Fig 5 gives the Doppler power averaged across the vessel lumen as a function of the flow rate for each experiment. Because different transmitted power and Doppler scan gain were used for each animal, comparisons cannot be made between blood samples. For all measurements, the power was minimum at high flow rates. As the flow rate was reduced, the power increased to reach a maximum at 125 mL/min for horses 1 and 2 and pig 1. For pig 2, the highest backscattered power was found at the flow rate of 75 mL/min. The range of variation of the Doppler scan power averaged across the vessel lumen was 8.7 dB for horse 1 and 9.4 dB for horse 2. The ranges of variation were lower for pig blood (6.1 dB for pig 1 and 3.6 dB for pig 2).

Fig 6 shows an example of the Doppler scan power (pig 2) as a function of the position across the vessel lumen for flow rates of 75, 250, and 1000 mL/min. For flow rates of 75 and 250 mL/min, the

Table II. Mean ± one standard deviation of the parameters v_{max}, n, and R of Equations 1 and 2

Flow rate (mL/min)	v_{max} *(cm/s)*	*n*	*R (mm)*
75	3.8 ± 1.1	2.6 ± 0.2	4.9 ± 0.2
125	5.5 ± 0.4	2.6 ± 0.1	4.7 ± 0.1
250	11.4 ± 1.8	2.2 ± 0.1	4.5 ± 0.1
500	21.6 ± 1.8	2.0 ± 0.1	4.6 ± 0.1
750	34.0 ± 2.1	2.0 ± 0.1	4.7 ± 0.1
1000	40.3 ± 2.6	1.9 ± 0.1	4.67 ± 0.04

v_{max}, Maximum centerline velocity; *n*, power law exponent; *R*, radius of the tube.
These parameters were used to estimate the velocity profile and the shear rate across the vessel lumen, at flow rates varying between 75 and 1000 mL/min. For each flow rate, the parameters were averaged over four experiments (horses 1 and 2, and pigs 1 and 2).

power was minimum close to the wall and maximum at a radial position of 0.8 mm, approximately. At these flow rates, the "black hole" was clearly seen at the center of the vessel. At the flow rate of 1000 mL/min, the power distribution across the vessel lumen was uniform. Although not reported, similar results were obtained for horses 1 and 2 and pig 1.

Effect of the shear rate on RBC aggregation. The model of Equation 1 was fitted to the velocity profiles measured experimentally. The parameters v_{max} and n were used to calculate, from Equation 2, the shear rate across the tube for all flow rates tested. Table II summarizes the values of these parameters and that of the estimated tube radius R. A blunted velocity profile (n > 2) was obtained for flow rates lower than 500 mL/min. The radius of the tube, estimated from the flow velocity images and the power law model of Equation 1, varied between 4.5 and 4.9 mm, which is close to the true radius of 4.76 mm. The influence of the shear rate on equine and porcine RBC aggregation is shown in Fig 7. For all experiments, the flow rate affected the way the shear rate influenced the Doppler scan power. At flow rates between 75 and 500 mL/min for equine blood and between 75 and 250 mL/min for porcine blood, the power increased at low shear rates, reached a maximum, and then decreased as the shear rate was further increased. The position of the peak of the Doppler scan power moved to higher shear rates as the flow rate was increased. For both equine and porcine blood, few power variations were observed as a function of the shear rate for flow rates of 750 and 1000 mL/min. The limited number of gray levels that is used, by this instrument, to map the backscattered power could have hidden the small

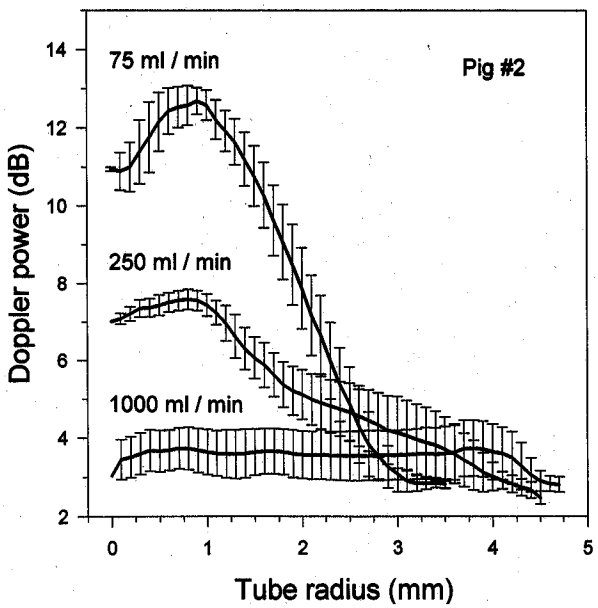

Fig 6. Example for pig 2 of cross-sectional distributions of Doppler scan power for flow rates of 75, 250, and 1000 mL/min. Results are expressed in terms of mean ± one standard deviation. These statistics were computed from all pixels located at radial position considered (radial increment of 0.5 mm was used). Radial position of 0 mm represents center of tube with radius of 4.76 mm.

power changes expected. For all experiments, no significant power variations were found beyond shear rates of 80 seconds^{-1}, independently of the flow rate. The largest power changes were measured for shear rates below 40 seconds^{-1}. The range of variation of the Doppler scan power as a function of the shear rate and flow rate was 17.6 dB for horses 1 and 2, 13.4 dB for pig 1, and 10.5 dB for pig 2.

DISCUSSION

RBC aggregation is a dynamic and reversible physiologic phenomenon occurring in flowing blood when macroproteins in the plasma are adsorbed on the RBC membrane to link RBCs as cylindrical rouleaux, branched rouleaux, and three-dimensional networks.[18,19] The mechanisms of rouleau formation and dissociation are complex and depend on the physiochemical properties of some plasma proteins, the deformability of RBCs, the repulsive negative electrical charges on the RBC membrane, the hematocrit, the temperature, the pH level, and the mechanical properties of the flow.[20-26] The physiopathologic significance of RBC aggregation is of several orders. RBC aggregation is a major

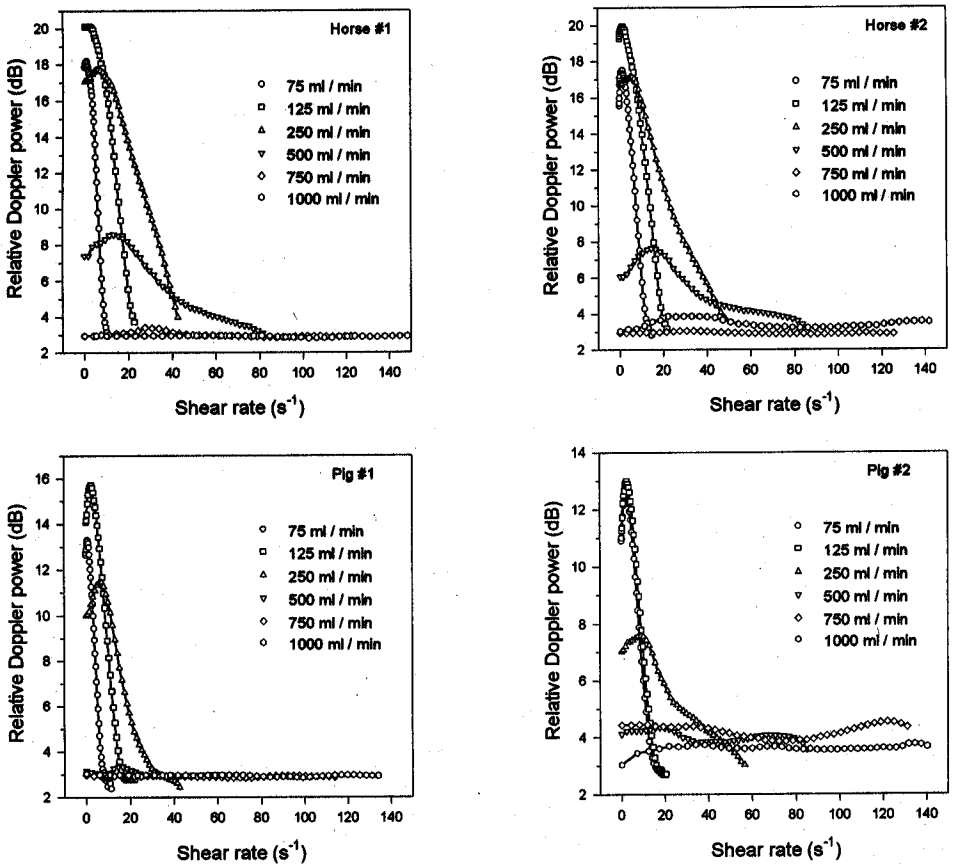

Fig 7. Relative Doppler scan power as function of shear rate across tube for equine and porcine whole blood. *Legends* give flow rate for each series of measurements. For clarity, only mean Doppler scan power values are shown in figure. Shear rate across tube was estimated at each radial position (increment of 0.5 mm was used) from Equation 2.

determinant of the viscosity of blood at low shear rates,[27] and, as a consequence, it affects the flow resistance. It also plays a role on the fluidity of blood in the microcirculation.[28,29] In the peripheral vasculature, high levels of RBC aggregation can induce flow stasis and have a direct effect on thrombotic venous disorders.[30-32] It may also have an indirect effect on the formation of arterial thrombi through its interaction with platelets[33,34] and leukocytes.[35]

Currently, no standardized method exists to measure RBC aggregation. However, several approaches were proposed to assess the level of RBC aggregation as a function of the shear rate. These methods involve blood viscosity measurements,[36] direct observations in shear flow with a microscope,[20] laser light transmission,[37] and reflection[38] measurements under shear conditions and after flow stoppage and ultrasound backscattering.[39] Because ultrasonic waves propagate through soft tissues and are only slightly attenuated in blood, the ultrasound backscattering method may allow the real-time and noninvasive in vivo characterization of RBC aggregation. Except for the ultrasound scan method, all other approaches necessitate the withdrawal of blood, the use of anticoagulant, and the analysis in a laboratory instrument. The development of imaging methods that allow the detection and characterization of RBC aggregation in situ in human vessels would be of major importance and would certainly stimulate prospective clinical studies aimed at elucidating the role of RBC aggregation in the development of cardiovascular disease. As shown in the present study, PDU can reach this objective and it may also help to improve our basic understanding of the relationship between the hemodynamic of the circulation and RBC aggregation in human vessels.

Interpretation of the results. In the present study, RBC aggregation affected both the velocity profiles and the gray level of PDU images. As seen

in Table II, blunted velocity profiles (n > 2) were found at flow rates varying between 75 and 250 mL/min because of the presence of aggregation. It is not surprising to see in Fig 7 that these flow rates corresponded to the highest levels of Doppler scan power observed. In the PDU image of Fig 4*A*, a reduction of the Doppler scan power at the center of the tube was found. This power drop, known as the "black hole" phenomenon, was previously detected on B-mode images[17,40] and PW Doppler scan measurements.[7,41] It is explained in the literature by the reduction of the level of RBC aggregation at the center of the tube. For instance, as first reported by Chien[42] and Copley et al,[43] the interaction (collisions) between RBCs gets stronger and RBC aggregation is enhanced as the shear rate is increased from zero (at the tube center) to some values. For shear rates above the rate producing the maximum aggregation, the dispersion of RBC aggregates begins and continues with increasing shear rates. It is interesting to observe that the results reported in Fig 7 show this behavior for flow rates of 250 mL/min and lower. The reason that the peak of the backscattered power moves to higher shear rates as the flow rate is increased was postulated to be related to the presence of an organized structure of the aggregates around the center of the tube.[41] The lowest power reported in Fig 5 for horses 1 and 2 and pig 1, at a flow rate of 75 mL/min, can be explained by the reduction in the size of the aggregates at very low shear rates (lower rate of collision between RBCs). For pig 2, no clear explanation is available for the absence of power reduction at 75 mL/min.

As reported in Table I, the kinetics of rouleau formation and the adhesive strength between RBCs were higher in equine blood than in porcine blood. The parameters measured with the erythroaggregameter were obtained by analyzing the scattered light intensity from RBCs and RBC aggregates flowing between two coaxial cylinders. The scattered light depends on the projected area of the particles and their orientation.[13] On the other hand, ultrasound scan backscattering, at a fixed hematocrit, is a function of the mean volume of the aggregates. Consequently, the results from both methods cannot be easily compared because different information is obtained, especially if nonsymmetrical 3D RBC aggregates are present. Moreover, the flow conditions were different. Nevertheless, a close relationship seems to exist between S_{10} or tA and the range of variation of the Doppler scan power observed for a given blood sample. For instance, in Fig 5, the ranges of variation of the Doppler scan power averaged across the vessel lumen as a function of the flow rate were higher in horses than in pigs (8.7 and 9.4 dB for horses vs 6.1 and 3.6 dB for pigs). In Fig 7, the ranges of variation as a function of the flow rate and shear rate were 17.6 and 17.6 dB for horses and 13.4 and 10.5 dB for pigs. As also seen in Fig 7, the shear rate corresponding to the complete disaggregation of RBCs was higher for horses than for pigs, which is consistent with the measured values of γS.

Practical considerations. The present study was performed with a commercially available ATL ultrasound scan system and an in vitro model. It was shown that the mapping of the backscattered power in gray level is logarithmic because PDU was originally designed to provide angiographic images. As seen in Fig 3, the range of power that can be displayed is limited to 20 dB, approximately. (The calibration procedure shown in Figs 2 and 3 was also performed with an Acuson 128 XP. Similar results were obtained. The mapping of the power was logarithmic, and the dynamic range was close to 20 dB.) Near the saturation of the PDU image, the sensitivity is poor and any variation in the backscattered power is displayed to a few gray levels. The best sensitivity to Doppler scan power variations would be obtained by adjusting the transmitted power and Doppler scan gain in a way to obtain gray levels just above the background noise that is mapped in black (if a gray color scale is used).

Other investigators believe that PDU is aliasing free and nearly angular independent when compared with CDF imaging.[1] The results seen in the Appendix show that PDU can be affected by frequency aliasing when the signal spectrum aliases into the wall filter. Moreover, in the presence of elongated scattering particles (carbon fibers suspended in a water-glycerol solution) and RBC aggregation, a study performed by our group[44] showed that the Doppler scan angle can also affect the backscattered power, which can be of interest. For instance, the angular variation of the backscattered power may be a way to assess the structure of the aggregates in human vessels. The absence of an angular variation may indicate no aggregation or clumps of RBCs, whereas changes in the backscattered power as a function of the angle may reflect elongated particles, such as rouleaux of RBCs. One limitation of the PDU imaging technique is its inability to measure RBC aggregation at complete and near stasis levels. However, as shown in the present study, this approach can provide measurements of the cross-sectional distribution of RBC aggregation under flowing condition. In a recent study,[45] differences in the level of RBC aggregation were detected between veins and arteries by analyzing the power, at the cen-

ter of the vessel, with the PW Doppler scan technique. These results may stimulate clinical studies aimed at evaluating the role of RBC aggregation in vascular thrombosis. However, before reaching this goal, the PDU mapping of the backscattered power should be made linear, provide measurements over a wider range of power variation, and be mapped with more gray levels. A hyperbolic power map may also be of relevance to emphasize the sensitivity of the technique to the presence of RBC aggregation.

In summary, a method made on the basis of PDU and CDF imaging was proposed to study the effect of the shear rate on RBC aggregation. The study was performed in vitro and should be validated in vivo because differences in the level of aggregation as a function of the shear rate may exist because of the effect of the temperature, pressure, pulsatility of the flow, and other unknown mechanisms. Power variations up to 17 dB (50 times on a linear scale) were measured across the tube and were attributed to changes in the level of RBC aggregation. The Doppler scan power was shown to be affected by the flow rate and the shear rate variations across the tube. For the four experiments reported, the largest power variations were measured for shear rates below 40 seconds^{-1}. No significant power variations were found for shear rates beyond 80 seconds^{-1}. Although the relationship between the shear rate and RBC aggregation was previously studied with other ultrasound scan methods, the present study shows the accuracy of PDU to provide such results. Compared with other methods, PDU has the advantage of being easily applicable to human or animal studies.

We thank Dr Helen Routh from Advanced Technology Laboratories for loaning us the ATL HDI-Ultramark 9 system used in this study. Acknowledgments are also addressed to Drs C. Tranulis and G. Soulez for reviewing the manuscript.

REFERENCES

1. Rubin JM, Bude RO, Carson PL, Bree RL, Adler RS. Power Doppler US: a potentially useful alternative to mean frequency-based color Doppler US. Radiology 1994;190:853-6.
2. Griewing B, Morgenstern C, Driesner F, Kallwellis G, Walker ML, Kessler C. Cerebrovascular disease assessed by color-flow and power Doppler ultrasonography. Comparison with digital subtraction angiography in internal carotid artery stenosis. Stroke 1996;27:95-100.
3. Steinke W, Meairs S, Ries S, Hennerici M. Sonographic assessment of carotid artery stenosis. Comparison of power Doppler imaging and color Doppler flow imaging. Stroke 1996;27: 91-4.
4. Wardlaw JM, Cannon JC. Color transcranial "power" Doppler ultrasound of intracranial aneurysms. J Neurosurg 1996;84:459-61.
5. Wu SJ, Reyner J, Shung KK, Routh HF. A study on the feasibility of using power level for detection of turbulence and vessel differentiation in Doppler power imaging. Ultrasonics Symposium Proceedings 1995;2:1527-30.
6. Cloutier G, Allard L, Durand LG. Characterization of blood flow turbulence with pulsed-wave and power Doppler ultrasound imaging. J Biomech Eng 1996;118:318-25.
7. Cloutier G, Qin Z. Shear rate dependence of normal, hypo-, and hyper-aggregating erythrocytes studied with power Doppler ultrasound. In: Lees S, Ferrari LA, editors. Acoustical imaging. New York: Plenum Press; 1997. p. 291-6.
8. Cloutier G, Qin Z. Ultrasound backscattering from non-aggregating and aggregating erythrocytes—a review. Biorheology 1997;34:443-70.
9. Shung KK, Thieme GA. Ultrasonic scattering in biological tissues. Boca Raton, Ann Arbor, London, Tokyo: CRC Press; 1993. p. 1-486.
10. Rickey DW, Picot PA, Christopher DA, Fenster A. A wall-less vessel phantom for Doppler ultrasound studies. Ultrasound Med Biol 1995;21:1163-76.
11. Milnor WR. Hemodynamics. Baltimore, Hong Kong, London, Sydney: Williams & Wilkins; 1989. p. 1-404.
12. Weng X, Cloutier G, Pibarot P, Durand LG. Comparison and simulation of different levels of erythrocyte aggregation with pig, horse, sheep, calf, and normal human blood. Biorheology 1996;33:365-77.
13. Donner M, Siadat M, Stoltz JF. Erythrocyte aggregation: approach by light scattering determination. Biorheology 1988;25:367-75.
14. Houbouyan LL, Delamaire M, Beauchet A, et al. Multicenter study of an erythro-aggregometer: quality control and standardization. Clin Hemorheol Microcirc 1997;17:299-306.
15. Hoskins PR, Loupas T, McDicken WN. A comparison of the Doppler spectra from human blood and artificial blood used in a flow phantom. Ultrasound Med Biol 1990;16:141-7.
16. Qin Z, Durand LG, Allard L, Cloutier G. Effects of a sudden flow reduction on red blood cell rouleau formation and orientation using RF backscattered power. Ultrasound Med Biol 1998;24:503-11.
17. Yuan YW, Shung KK. Echoicity of whole blood. J Ultrasound Med 1989;8:425-34.
18. Samsel RW, Perelson AS. Kinetics of rouleau formation. II. Reversible reactions. Biophys J 1984;45:805-24.
19. Fabry TL. Mechanism of erythrocyte aggregation and sedimentation. Blood 1987;70:1572-6.
20. Schmid-Schönbein H, Gaehtgens P, Hirsch H. On the shear rate dependence of red cell aggregation in vitro. J Clin Invest 1968;47:1447-54.
21. Jan KM, Chien S. Role of surface electric charge in red blood cell interactions. J Gen Physiol 1973;61:638-54.
22. Skalak R. Aggregation and disaggregation of red blood cells. Biorheology 1984;21:463-76.
23. Neumann FJ, Schmid-Schönbein H, Ohlenbusch H. Temperature-dependence of red cell aggregation. Pflugers Arch 1987;408:524-30.
24. Maeda N, Seike M, Suzuki Y, Shiga T. Effect of pH on the velocity of erythrocyte aggregation. Biorheology 1988;25: 25-30.

25. Deng LH, Barbenel JC, Lowe GDO. Influence of hematocrit on erythrocyte aggregation kinetics for suspensions of red blood cells in autologous plasma. Biorheology 1994;31:193-205.
26. Weng X, Cloutier G, Beaulieu R, Roederer GO. Influence of acute-phase proteins on erythrocyte aggregation. Am J Physiol 1996;271:H2346-52.
27. Chien S. Biophysical behavior of red cells in suspensions. In: Surgenor DM, editor. The red blood cell. New York, San Francisco, London: Academic Press; 1975. p. 1031-133.
28. Schmid-Schönbein H, Gallasch G, Volger E, Klose HJ. Microrheology and protein chemistry of pathological red cell aggregation (blood sludge) studied in vitro. Biorheology 1973;10:213-27.
29. Schmid-Schönbein H. Critical closing pressure or yield shear stress as the cause of disturbed peripheral circulation? Acta Chir Scand 1976;465:10-9.
30. Chabanel A, Horellou MH, Conard J, Samama MM. Red blood cell aggregability in patients with a history of leg vein thrombosis: influence of post-thrombotic treatment. Br J Haematol 1994;88:174-9.
31. Zuccarelli F, Taccoen A, Razavian M, Chabanel A. Increasing erythrocyte aggregability with the progressive grades of chronic venous insufficiency: importance and mechanisms. J Cardiovasc Surg 1995;36:387-91.
32. Kwaan HC, Levin M, Sakurai S, et al. Digital ischemia and gangrene due to red blood cell aggregation induced by acquired dysfibrinogenemia. J Vasc Surg 1997;26:1061-8.
33. Koenig W, Ernst E. The possible role of hemorheology in atherothrombogenesis. Atherosclerosis 1992;94:93-107.
34. Tanahashi N, Tomita M, Kobari M, et al. Platelet activation and erythrocyte aggregation rate in patients with cerebral infarction. Clin Hemorheol 1996;16:497-505.
35. Pearson MJ, Lipowsky HH. Red cell aggregation induced leukocyte margination [abstract]. Ann Biomed Eng 1998; 26:S30.
36. Brooks DE, Goodwin JW, Seaman GVF. Interactions among erythrocytes under shear. J Appl Physiol 1970;28:172-7.
37. Schmid-Schönbein H, Volger E, Klose HJ. Microrheology and light transmission of blood. II. The photometric quantification of red cell aggregate formation and dispersion in flow. Pflugers Arch 1972;333:140-55.
38. Mills P, Adler P, Dufaux J, Quemada D. Étude de l'agrégation d'une suspension sanguine par rétrodiffusion laser. J Mal Vasc 1979;4:91-4.
39. Sigel B, Machi J, Beitler JC, Justin JR, Coelho JCU. Variable ultrasound echogenicity in flowing blood. Science 1982; 218:1321-3.
40. Shehada REN, Cobbold RSC, Mo LYL. Aggregation effects in whole blood: influence of time and shear rate measured using ultrasound. Biorheology 1994;31:115-35.
41. Qin Z, Durand LG, Cloutier G. Kinetics of the "black hole" phenomenon in ultrasound backscattering measurements with red blood cell aggregation. Ultrasound Med Biol 1998;24:245-56.
42. Chien S. Electrochemical interactions between erythrocyte surfaces. Thromb Res 1976;8:189-202.
43. Copley AL, King RG, Huang CR. Erythrocyte sedimentation of human blood at varying shear rates. In: Grayson J, Zingg W, editors. Microcirculation. New York: Plenum Press; 1976. p. 133-4.
44. Allard L, Cloutier G, Durand LG. Effect of the insonification angle on the Doppler backscattered power under red blood cell aggregation conditions. IEEE Transactions on Ultrasonics, Ferroelectrics, and Frequency Control 1996;43:211-9.
45. Cloutier G, Weng X, Roederer GO, Allard L, Tardif F, Beaulieu R. Differences in the erythrocyte aggregation level between veins and arteries of normolipidemic and hyperlipidemic individuals. Ultrasound Med Biol 1997;23:1383-93.

Submitted Oct 20, 1998; accepted Jan 19, 1999.

APPENDIX

It is generally assumed that PDU is aliasing free.[1] For this reason, it may be advantageous when tissue motion is negligible to set the PRF of the Doppler ultrasound scan system as low as possible to increase the image sensitivity. Moreover, because the lowest wall filter frequency that can be selected depends on the PRF for the ATL system, it may also be necessary to use a low PRF to reduce the effect of the wall filter on the Doppler scan signal. However, we found that frequency aliasing can produce artifacts on PDU images that may affect the quantification of blood echogenicity. The following results are presented to show conditions that produce artifactual PDU images.

The flow model described in the Methods section was used. The test fluid was a solution of water/glycerol (70%/30%) and 0.5 g/L of superfine Sephadex particles. All recordings were performed at a steady flow rate of 600 mL/min and a Doppler scan angle of 70 degrees. With these experimental conditions, a PRF of 600 Hz was necessary to avoid frequency aliasing. Fig 8 shows the PDU and CDF images recorded with a PRF of 450 Hz and a wall filter frequency of 25 Hz. Frequency aliasing was observed on the CDF image (Fig 8*B*) around the center of the vessel. This frequency aliasing artifact also produced a reduction of the Doppler scan power around the tube center (Fig 8*A*). To emphasize this artifact, the PRF was not changed, but the wall filter frequency was increased to 100 Hz. As

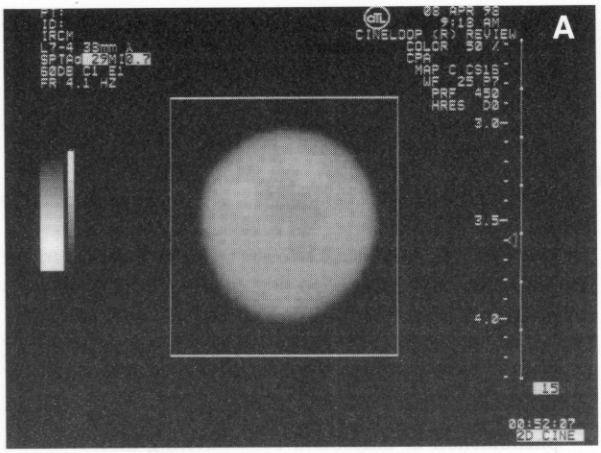

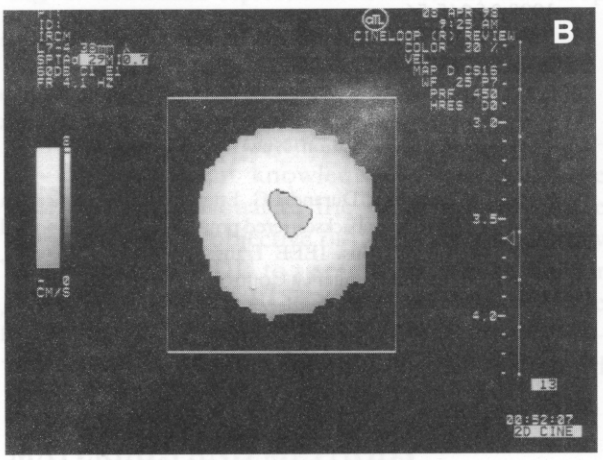

Fig 8. Power Doppler scan **(A)** and color Doppler scan flow **(B)** images recorded at steady flow rate of 600 mL/min and Doppler scan angle of 70 degrees. Test fluid was solution of water/glycerol (70%/30%) and 0.5 g/L of superfine Sephadex particles. PRF was set to 450 Hz to produce frequency aliasing (PRF of 600 Hz was necessary to avoid aliasing), and wall filter frequency was 25 Hz. Frequency aliasing artifact is seen on both power and color flow images.

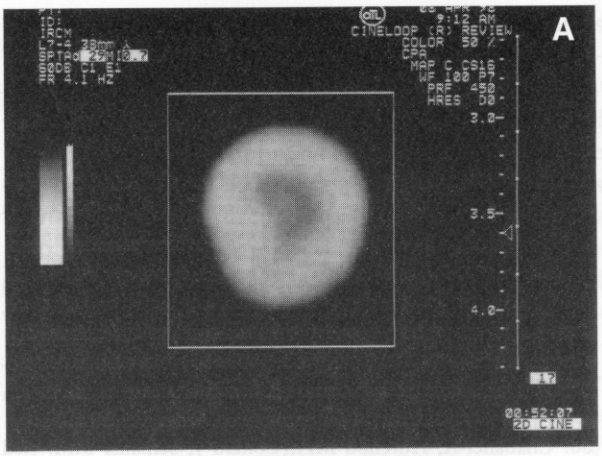

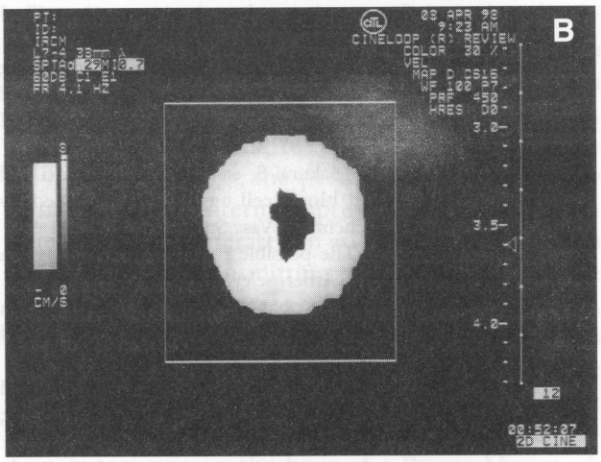

Fig 9. Figure shows same technique as Fig 8, but wall filter frequency was increased to 100 Hz to emphasize frequency aliasing artifact on power **(A)** and color flow **(B)** images.

shown in Fig 9, the frequency aliasing artifact now removed almost all the Doppler scan signal around the center of the tube. This affected both the PDU (Fig 9*A*) and the CDF (Fig 9*B*) images.

By varying the PRF, the flow rate, or both, the visual aspect of the frequency aliasing artifact changed from a hole at the center of the tube to a ring within the vessel lumen. In Figs 8 and 9, it would be possible to misleadingly associate this artifact to the "black hole" phenomenon.[17] For blood echogenicity measurements, the PRF should be selected high enough to avoid frequency aliasing. As the PRF is dropped and aliasing occurs, the high velocities are wrapped around to fall within the wall filter and therefore appear to be of lower power. As mentioned in the introduction, PDU is mostly used to produce angiographic images of blood flow. It is usually applied to detect low flow in the microcirculation. Because frequency aliasing may not occur at low flow, it is recommended to use a low PRF for this application. However, if the flow becomes high enough to produce aliasing, this artifact may result in an apparent lack of blood perfusion because of the disappearance of the vessel on the image.